Available online at www.sciencedirect.com

ScienceDirect

Procedia Manufacturing 35 (2019) 795–801

Procedia MANUFACTURING

www.elsevier.com/locate/procedia

2nd International Conference on Sustainable Materials Processing and Manufacturing

(SMPM 2019)

Commuting Tillage Operations of HRP under Hydraulic Cylinder Movements on Plough-breast Performance

Min Wei[a], Lin Zhu[a*], Feng Luo[a], Jia-Wen Zhang[a], Tien-Chien Jen[a,b*]

[a]*Mechanical Engineering Department, Anhui Agricultural University, Hefei, 230036, P. R. China*
[b] *Mechanical Engineering Science Department, University of Johannesburg, Johannesburg, 2006, South Africa*

Abstract

Hydraulic Cylinder (HC) is used for the commuting tillage of Horizontally Reversible Plough (HRP). Although the commuting behaviors are demonstrated not to affect basic beam of HRP, whether it has adverse effects on the essential engaging components of HRP, i.e. moldboard is unknown. This study addressed the estimation of the HC movements on the mouldboard, and particularly on the plough-shank of the plough-breast. A combined finite element analysis (FEA), multi-body dynamics analysis (MDA), and scanning electron microscope (SEM) based measurements was applied for five different HC movement scenarios and two actual HRP tilling conditions at the maximum operation depth, i.e. 0.36m. The results demonstrate that the HC movements produce both the maximum stress & strain and the most severe abrasion wear at the plough-shank, but they have no significantly adverse effects on the service life of the plough-breast. The current HC absolutely favors the actual HRP tillage.

Peer-review under responsibility of the organizing committee of SMPM 2019.

Keywords: Commuting; Finite element analysis (FEA); Hydraulic Cylinder (HC); Multi-body dynamics analysis (MDA); Plough-shank

1. Introduction

HRP, developed by Xin-Jiang Agricultural Mechanization Institute (XJAMI) of China, is a novel moldboard plough. The distinguished advantage of HRP, compared with the regular moldboard plough, is that it is able to perform a continuous and alternative high-speed commuting tillage with excellent operation performances (such as steady tilling and orderly soil cutting), as shown in Fig.1.

For the purpose of the commuting tillage, a small-cubage hydraulic cylinder (HC) is applied for HRP. During the HRP tillage, HC is used to compel Basic Beam (BB) to rotate with respect to Main Beam (MB), and then BB drive the plough body to implement the HRP commuting tillage. Figure 2 illustrates two different tillage processes

* Corresponding author. Tel.:+86-13696544372. Prof Zhu and Prof Jen are co-corresponding authors
E-mail address: zl009@mail.ustc.edu.cn; tjen@uj.ac.za

2351-9789
Peer-review under responsibility of the organizing committee of SMPM 2019.
10.1016/j.promfg.2019.06.025

of HRP, and n indicates the rotational speed of BB with respect to MB. More generally, the varying HC movements are believed to adversely affect the components of HRP, e.g. BB. For this reason, we conducted the dynamics behaviors of BB and optimized the motion type of HC, demonstrating that uniform motion applied for HC favors HRP, and that the dynamic impact due to the uniform motion has no detrimental effects on the service life of BB [1]. However, there still exists another question whether the commuting loads have an adverse effect on the two essential engaging components of HRP, i.e. ploughshare and moldboard (Fig.3). Currently, so severe worn land is demonstrated to lie at the plough-shank of the plough-breast after HRP is operated for a certain period, which shortens the service life of moldboard. This study is therefore aimed to the commuting effects on the plough-breast.

Fig.1. HRP working in the field

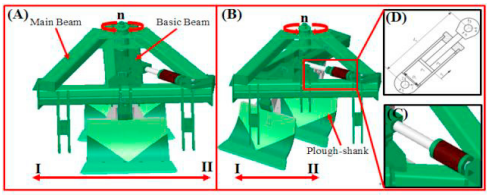

Fig.2. (A) The first and (B) second commuting tillage processes of HRP, HC with (C) magnified view and (D) main dimensions

2. Materials and Methods

2.1. Geometric model

For 3D HRP modeling purpose, feature-based modeling approach incorporating virtual assembly technology (VAT) was used in commercial software, i.e. SolidWorks. The detailed information is depicted as follows: firstly, the 3D models of parts and components were constructed with feature-based modeling approaches; then, Virtual Assembly Technology (VAT) was employed for assembling HRP; finally, interference check technique (ICT) was used for verification of the 3D HRP model (Fig.2). Detailed geometrical data of HRP are available in [3], where the overall dimensions of HRP are 2.8 m length, 2.35 m width and 1.2 m height, respectively [1].

2.2. Multi-body dynamics and finite element analysis

In this section, firstly, MDA is implemented to investigate the dynamics behaviors of the plough-breast with the five different HC speeds under the two different HRP tillage scenarios; then, the resulting MDA load data are transferred to the related FE model for predicting the stress and strain variations on the plough-breast under various HC movements. Note that the maximum operation depth was considered for all numerical simulations in this study. It is because the maximum operation depth is associated with the most violent soil/tool interaction [4].

2.2.1.Multi-body dynamics analysis

The three-dimensional model of HRP, previously constructed in Fig.2, was imported into MSC ADAMS motion software (Santa, Ana, CA, USA) in preparation for a multi-body dynamics analysis. Newton-Laphson iteration approach was used to numerically analyze the performance characteristics of RM, especially of various HC movements, and then the loads acting on the plough-breast. This calculation is based on the practical tillage behaviors of HRP. During the HRP tillage, the moving parts of RM are, respectively, basic beam (BB), hydraulic cylinder (HC) and reversing rod (RR); the immovable part is main beam (MB). The tillage behavior is varied with the HC velocities, which are specified from 15 to 25mm/s in 2.5 mm increments.

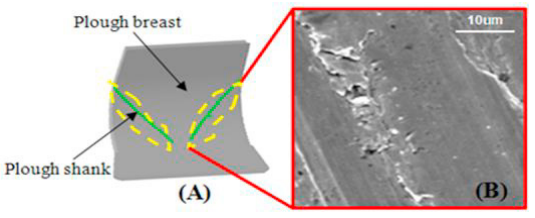

Fig.3. (A) moldboard of HRP (B) SEM micrographs of the worn Plough-breast surface at tool speed 6km/h and operation depth 0.27m after 50

Fig.4 Meshed plough-breast

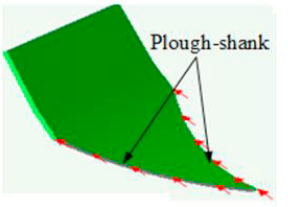

Fig.5 Loaded plough-breast

2.2.2. Finite element analysis

The three-dimensional model of plough-breast developed for the MDA was imported into ANSYS 11 mechanical (ANSYS, Inc., Canonsburg, PA, USA) in preparation for FEA. In order to obtain accurate numerical simulation results, the strategy in this study was based on high-density mesh, in which each solid element has ten nodes for regions requiring high resolution. Four-point Jacobian check method for the distortion level of tetrahedral elements was utilized to mesh the entire plough-breast (Fig.4). It is pointed out that 4773 elements and 1705 nodes were used for the tool. Besides, according to the practical application, the plough-breast herein was modeled as alloy steel material with a Young's modulus of 210 GPa and a Poisson's ratio of 0.3 [2]. Figure 5 schematically shows the loaded plough-breast.

2.3. Field experiments

For simulations validating purpose, in the April of 2018 the experimental part of this study took place at a farm of Hutu-bi County of Xinjiang of China, where the soil properties are identified with those for numerical predictions. In order to reduce the influence of soil condition variation during measurements, the test plot was thoroughly ploughed to a specified depth, i.e. 0.360 m and harrowed to consolidate until forty-nine-hour tillage operations were finished before the measurement (Fig.6). The measurements on wear morphology were implemented by a scanning electron microscope (SEM) (Regulus 8100, HITACHI, Japan) at public experimentation center of Anhui Agricultural University (Fig.7).

For the entire test, the wear morphology at the plough-shank zone was measured for five times with a stereoscopic microscope (maximum 50-fold magnification). This microscope was connected to an image acquisition system consisting of a CCD camera and a computer with image acquisition software. The images of the worn plough-breast were recorded in the scanning electron microscope (SEM) to further understand the tool wear behavior.

Fig.6 HRP testing in the field

Fig.7 SEM used for wear morphology

3. Results

3.1. MDA and FEM based load predictions

3.1.1 Load variations by using MDA

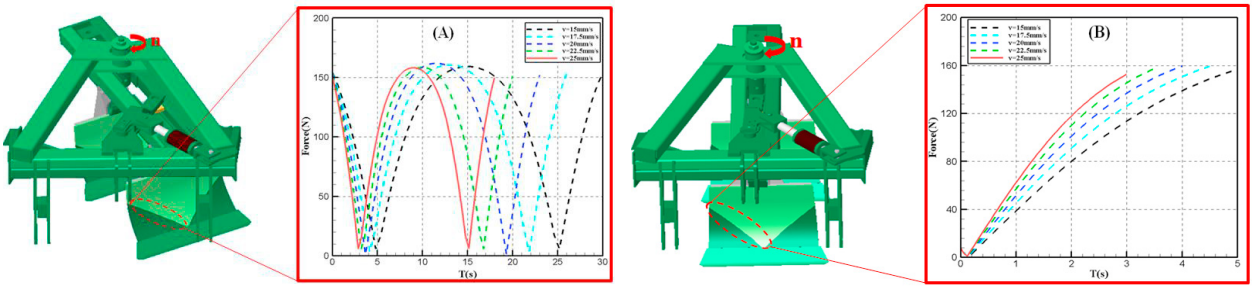

Fig.8 Plough-shank force data in the (A) first and (B) second tillage process plotted vs. tillage time

Figure 8 shows the load variations across the plough-shank with tillage time by using MDA. These force data were calculated based on the combined five different HC speeds and two different HRP tillage scenarios.

As observed in the first tillage scenario, with the HC speed increase the maximum load is first increased, i.e. from 160 N at 15 mm/s to 165 N at 20 mm/s and then is decreased to approximate 160 N at 25mm/s. In the second tillage scenario, the maximum load is also first increased, i.e. from 158 N at 15 mm/s to 160 N at 20 mm/s and then is decreased to approximate 158 N at 25mm/s. This can be explained as follows: with HC speed increase the interaction between soil and plough-shank becomes severer, however, when the HC movement is too fast, the foregoing effect may decrease because of rapid soil flow pattern and, consequently, the reduction in the contact area between soil and plough-shank. Note that the load between soil and tool consists of compression and shear interactions, as shown in Fig.5. In the practical applications of HRP, the main engagement between soil and plough-breast occurs at the plough-shank, where so much energy contributes to cutting, breaking down, inverting soil layers and rearranging aggregates [5-7].

3.1.2. Load predictions by using FEA

In this section, the Finite Element predictions are concerned with Von Mises stress and strain on the plough-breast and especially on the plough-shank. Note that due to the structural symmetry of plough-breast, the maximum stress and strain at the left plough-shank are only presented here (Fig.8).

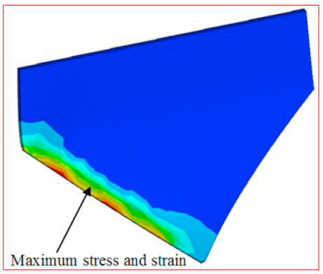

Fig.9.Maximum stress and strain on the plough-shank under the two different HRP tillage scenarios

Figure 9 show the maximum Von Mises stress and strain distributions across at the plough-shank section in the either first or the second tillage scenario. Our finding is that in the identified range of HC speeds there is reasonably good qualitative agreement in the maximum von Mises stress and strain distribution under all HRP tilling scenarios. That is, the FE based predictions have the same stress & strain profile distributions. This is likely due to the same tillage performances of the plough-shank in the practical HRP operations (Fig.8). However, there is also a discrepancy in magnitude for the maximum Von Mises stress and strain under the two different tiling scenarios. The detailed values are seen in Table 1.

Table 1. Maximum Von Mises stress/strain under the five different HC speeds in the two different tillage scenarios

Items	tillage scenario I	tillage scenario II
V=15.0 mm/s	591.8MPa/2.82×10^{-9}	582.6Pa/2.77×10^{-9}
V=17.5 mm/s	597.1MPa/2.84×10^{-9}	592.2Pa/2.82×10^{-9}
V=20.0 mm/s	602.3MPa/2.87×10^{-9}	592.3Pa/2.82×10^{-9}
V=22.5 mm/s	589.0MPa/2.81×10^{-9}	584.9Pa/2.79×10^{-9}
V=25.0 mm/s	587.8MPa/2.80×10^{-9}	567.4Pa/2.70×10^{-9}

As observed, all of the maximum stress & strain at the plough-shank vary as the change in HC speed. For the first tillage scenario, the greatest stresses & strains at the plough-shank are 591.8Pa/2.82×10^{-9}, 597.1Pa/2.84×10^{-9}, 602.3Pa/2.87×10^{-9}, 589.0Pa/ 2.81×10^{-9} and 587.8Pa/2.80×10^{-9}, respectively, corresponding to 15, 17.5, 20, 22.5 and 25mm/s. For the second tillage scenario, in the same HC-speed range as above, the greatest stresses & strains at the plough-shank are 582.6Pa/2.77×10^{-9}, 592.2Pa/2.82×10^{-9}, 592.3Pa/2.82×10^{-9}, 584.9Pa/2.79×10^{-9} and 567.4Pa/2.70×10^{-9}, respectively. This can be explained as follows:

1) In the continuous, alternative, and commuting tillage operations of HRP, a majority of the soil enters the plough-breast surface by way of the intermittent section of the plough-shank. This phenomenon indicates that the primary soil engagement zone on the plough-breast is the plough-shank, where the violent soil-tool interaction generally happens to finish cutting, breaking down, and inverting the soil layers.

2) For the two different HC tillage scenarios, when the HC speed is increased from 15 to 25 mm/s, the maximum load on the plough-shank is increased by the more violent soil-tool interaction; however, with further increasing HC speed, the contact time between soil and plough-shank is becoming shorter, which leads to the lower contact length (or contact area) and hence the reduced maximum stress & strain at the plough-shank.

3.2. Tool wear morphology

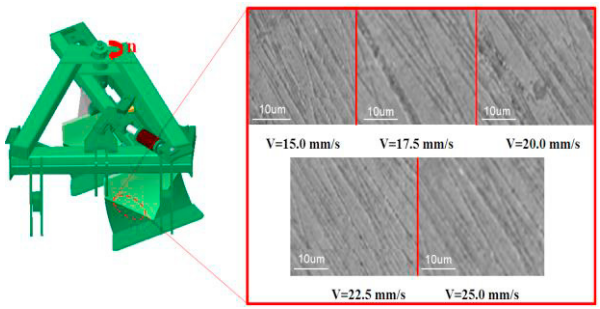

Fig.10. SEM views of the plough-shank in the first tillage process

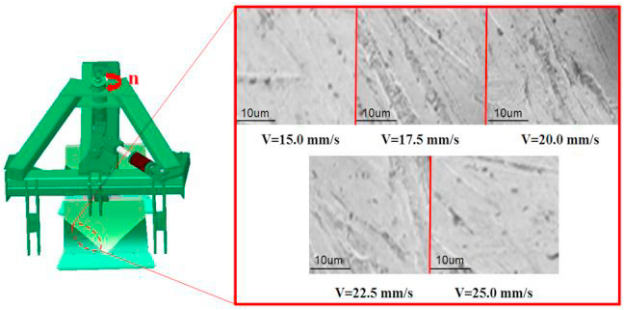

Fig.11. SEM views of the plough-shank in the first tillage process

Soil-tillage interaction is a significantly complex soil cutting process, involving a high rate of plastic deformation and soil failure characterized by the flow of soil particles. More generally, it is the abrasion with hard soil particles involved during cutting that incurs severe worn land on the plough-surface, e.g. on the plough-shank of the plough-breast. Consequently, this dynamic interaction has strong effects on the tool life. Hence, in the experiments several different wear mechanisms were identified dependent on the various HC speeds and the maximum operational depth using the scanning electron microscope. Note that the SEM based measurements were focused on the intermittent section of the plough-shank because a majority of the soil enters the plough-breast surface by way of the intermittent section of the plough-shank.

Figures 10-11 show the detailed structural characterization at the plough-shank zone of the plough-breast, at the three different operational depths and the constant tool speed, by using a scanning electron microscope (SEM). From these pictures, we can see that all the worn land variations change with the HC speed. For the first tillage scenario, the severe worn land is becoming more severe with the HC speed increase and then gradually relief; the most severe worn land appears at the HC speed of 20 mm/s. For the second tillage scenario, the most severe worn land is also

observed at the HC speed of 20 mm/s. In this regard, it is observed that the overall trend of the numerical results is in good qualitative agreement with that of the measured evidences in the field.

4. Conclusions

A combination of MDA & FEA based numerical investigations and SEM based experimental measurements have been implemented to examine the effects of HRP commuting tillage operations due to the HC movements on the plough-breast Performance. It has investigated the soil/plough-breast dynamics interaction characteristics associated with five HC speeds (15, 17.5, 20, 22.5, and 25 mm /s) and the maximum operational depth (0.360 m). Evaluation has been done primarily with respect to the two actual HRP tilling conditions, i.e. commuting between left and right/ middle continuously and alternatively for the soil load acting on the plough-breast and tool wear morphology.

The varying HC movements have been found to have influences on the dynamics interaction between soil and plough-breast. From the simulation and experiment, the maximum load and the most severe abrasion wear due to the HC movements both appear at the plough-shank, especially at its intermediary area, and the maximum load and most severe worn land are both observed at the HC speed of 20 mm/s. In terms of the relation between the dynamics interaction load and the tool surface morphology, there is qualitative agreement between simulation and experiment at the identified tillage conditions.

Previous experimental and computational studies have demonstrated that the highest stress by the draught force is located at the plough-shank of the plough-breast during HRP tillage [2]. The maximum stress calculated was 62.81MPa. However, for all numerical simulations in this study, the maximum stress due to dynamic effect of HC movements is approximate 602.2Pa. Compared with the previous result, the magnitude in the maximum stress by HC movement is too small; and moreover, the ultimate strength of the material used for plough-breast, i.e. alloy steel is 723.8MPa [2]. Consequently, the maximum stress due to HC movements can be negligible at all. Hence, the mechanics of commuting due to the HC movements does not affect the tillage performance of the plough-shank, and hence, shorten the tool life. This finding suggests that the various movements of HC under the two different tillage scenarios have no adverse effects on the service life of the plough-breast, and that the selected motion type of HC, i.e. uniform motion, absolutely favors the commuting tillage of HRP.

Acknowledgments

The authors thank the reviewers for their hard work. And also the authors acknowledge financial support for this work from the National Natural Science Foundation of China (Grant No. 51575003), Anhui Provincial Natural Science Foundation (Grant No.1508085ME71) and Key Project of Anhui Education Committee (Grant No. KJ2015A031).

References

[1] Lin Zhu, Chen-Long Yin, Fa Chen, The Application of virtual prototype Reversible Plow, International Journal of the Japan Society of Mechanical Engineering, Series. C, 41(2006) 247–252.

[2] Lin Zhu, Cheng-Long Yin, Fan-Rang Kong, Li Guo, Xiao-Ming Sun, Finite Element Analysis for Plough-breast of Horizontal Reversible Plow, Journal of system simulation.19 (17) (2007) 3934–3936.

[3] Lin Zhu, Shuang-Shuang Peng, Xi-Cheng, Yin-Yin Qi, Wen-Feng Zhang, Liang-Yuan Xu. Virtual assembly geometric semantics and constraint for an improved three-dimensional model of Horizontally Reversible Plow. International Journal of Mechanical Science and Technology (2016).

[4] Natsis, A., Petropoulos, G., Pandazaras, C., Influence of local soil conditions on mouldboard ploughshare abrasive wear, Tribology International. 41(2008) 151–157.

[5] Shmulevich, I., State of the art modeling of soil-tillage interaction using discrete element method, Soil & Tillage Research.111(2010) 41-53.

[6] Okayasu T., Morishita, K., Terao, H., Mitsuoka, M., Inoue, E., Fukami, K.O., Modeling and prediction of soil cutting behavior by a plow. In: CIGR-AgEng, Int. Conf. Agricult. Eng., “Agriculture & Engineering for a Healthier Life”, pp. 23, Valencia, July 8-12. (2012) ISBN-10:84-615-9928-4.

[7] A.E.Farid Eltom, Weimin Ding, Qishuo Ding, Abu baker B. Ali, B.Eisa Adam, Effect of trash board on moldboard plough performance at low speed and under two straw conditions, International Journal of Terramechanics.59(2015) 27–34.

[8] Gill, W.R., Vanden Berg, G.E., Soil dynamics in tillage and traction. In: Agriculture Handbook No. 316. Agricultural Research Service, U.S. Department of Agriculture.511(1967).

[9] Koolen A J, Agricultural Soil Mechanics. Advanced Series In Agricultural Sciences. Springer-Verlag, Berlin (1983).